Article

Cell Reports

Deletion of Human *tarbp2* Reveals Cellular MicroRNA Targets and Cell-Cycle Function of TRBP

Graphical Abstract

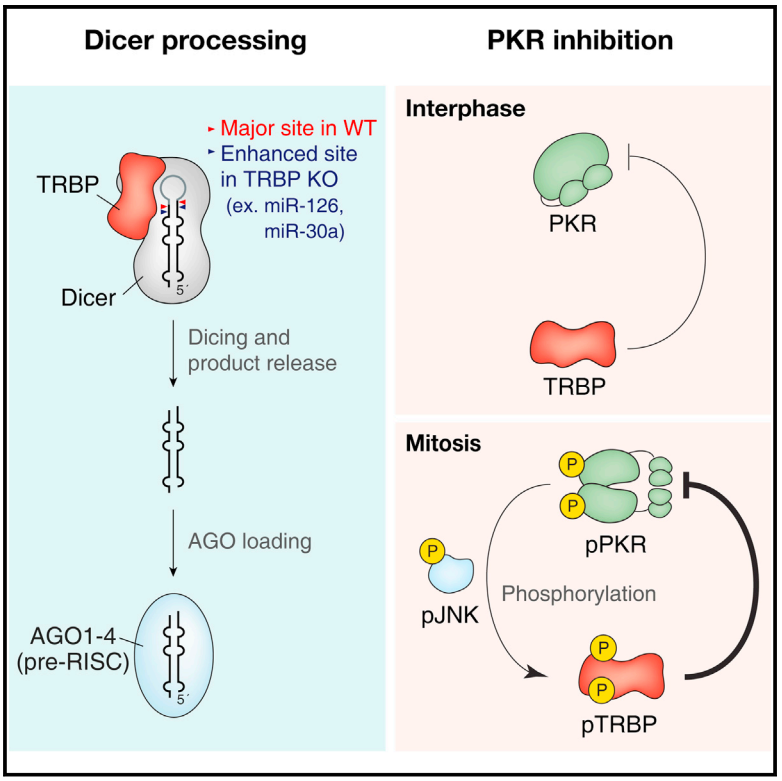

Authors

Yoosik Kim, Jinah Yeo, ..., Jong-Seo Kim, V. Narry Kim

Correspondence

narrykim@snu.ac.kr

In Brief

Kim et al. generate TRBP KO HeLa cells to investigate the cellular functions of TRBP. TRBP regulates the accuracy of Dicer processing for a subset of miRNAs without affecting their global abundance. They also identify hyperphosphorylation of TRBP in M phase, which augments inhibition of PKR in M-G1 transition.

Highlights

TRBP depletion affects the accuracy of Dicer processing for a subset of miRNAs

TRBP and PACT do not regulate miRNA abundance, Ago loading, or strand selection

TRBP is hyperphosphorylated by JNK during mitosis

Hyperphosphorylation enhances the inhibitory activity of TRBP on PKR

Accession Numbers

GSE61458

Kim et al., 2014, Cell Reports 9, 1061–1074
November 6, 2014 ©2014 The Authors
http://dx.doi.org/10.1016/j.celrep.2014.09.039

Cell Reports
Article

Deletion of Human *tarbp2* Reveals Cellular MicroRNA Targets and Cell-Cycle Function of TRBP

Yoosik Kim,[1,2,3] Jinah Yeo,[1,2,3] Jung Hyun Lee,[1,2,3] Jun Cho,[1,2] Daekwan Seo,[1,2] Jong-Seo Kim,[1,2] and V. Narry Kim[1,2,*]
[1]Center for RNA Research, Institute for Basic Science, Seoul 151-742, South Korea
[2]School of Biological Sciences, Seoul National University, Seoul 151-742, South Korea
[3]Co-first author
*Correspondence: narrykim@snu.ac.kr
http://dx.doi.org/10.1016/j.celrep.2014.09.039

SUMMARY

TRBP functions as both a Dicer cofactor and a PKR inhibitor. However, the role of TRBP in microRNA (miRNA) biogenesis is controversial and its regulation of PKR in mitosis remains unexplored. Here, we generate TRBP knockout cells and find altered Dicer-processing sites in a subset of miRNAs but no effect on Dicer stability, miRNA abundance, or Argonaute loading. By generating PACT, another Dicer interactor, and TRBP/PACT double knockout (KO) cells, we further show that TRBP and PACT do not functionally compensate for one another and that only TRBP contributes to Dicer processing. We also report that TRBP is hyperphosphorylated by JNK in M phase when PKR is activated by cellular double-stranded RNAs (dsRNAs). Hyperphosphorylation potentiates the inhibitory activity of TRBP on PKR, suppressing PKR in M-G1 transition. By generating human TRBP KO cells, our study clarifies the role of TRBP and unveils negative feedback regulation of PKR through TRBP phosphorylation.

INTRODUCTION

Transactivation response element RNA-binding protein (TRBP) was originally identified as a protein that binds to the RNA of human immunodeficiency virus type 1 and enhances its translation and replication (Dorin et al., 2003; Gatignol et al., 1991, 1996). TRBP is a double-stranded RNA (dsRNA)-binding protein with three dsRNA-binding domains (dsRBDs), two of which are highly conserved. TRBP recognizes secondary structure on RNAs with its two N-terminal dsRBDs (dsRBD1 and dsRBD2; Daviet et al., 2000). The third C-terminal dsRBD (dsRBD3) does not bind to RNAs but mediates protein-protein interaction to Merlin, Dicer, and protein activator of the interferon-induced protein kinase (PACT) in an RNA-independent manner (Haase et al., 2005; Laraki et al., 2008; Lee et al., 2004, 2006).

TRBP is a multifaceted protein with two well-characterized functions (Daniels and Gatignol, 2012; Gatignol et al., 2005). It is an integral component of Dicer-containing complexes and assists Dicer in generating small RNA-induced silencing complex (RISC) (Chendrimada et al., 2005; Haase et al., 2005; MacRae et al., 2008). Dicer is a key component in the biogenesis of ~22 nt long small noncoding RNAs called microRNAs (miRNAs) that negatively regulate complementary target mRNAs (Ha and Kim, 2014). The canonical miRNA biogenesis pathway consists of two sequential processing reactions of a primary transcript by RNase III enzymes (Lee et al., 2002). Drosha, together with DGCR8, cleaves the primary transcript into ~65 nt long precursor with a stem loop structure (Denli et al., 2004; Gregory et al., 2004; Han et al., 2004; Landthaler et al., 2004; Lee et al., 2003). The resulting precursor miRNA (pre-miRNA) is then recognized by Dicer-TRBP complex, which produces ~22 nt mature miRNA duplex (Bernstein et al., 2001; Grishok et al., 2001; Hutvágner et al., 2001; Ketting et al., 2001; Knight and Bass, 2001). One strand of the duplex is then loaded onto Argonaute (Ago) protein to induce RNA silencing (Hammond et al., 2001; Mourelatos et al., 2002; Tabara et al., 1999).

Through the dsRBD3, TRBP interacts with the region between DEXH and helicase domain of Dicer (Daniels et al., 2009; Lee et al., 2006). It has been reported that this interaction stabilizes Dicer and that knockdown of TRBP results in decreased expression of miRNAs (Chendrimada et al., 2005; Melo et al., 2009). However, the role of TRBP in Dicer stabilization and pre-miRNA processing is rather controversial, as other studies failed to reproduce such effects (Haase et al., 2005; Lee et al., 2006). Through in vitro reconstitution system, it has been demonstrated that, without TRBP, the accuracy of Dicer cleavage is compromised, leading to generation of truncated iso-miRs (Lee and Doudna, 2012). The tuning of the miRNA length by Dicer cofactors has been also demonstrated in mouse and fly systems where depletion of TRBP or Loquacious (Loqs), a fly homolog of TRBP, resulted in generation of shorter iso-miRs (Fukunaga et al., 2012). However, analysis of human TRBP in cellular level is currently lacking and TRBP-sensitive cellular miRNAs remain to be identified.

In addition to Dicer processing, TRBP can regulate the loading of Dicer cleavage products onto Ago during RISC assembly. It was first demonstrated in *Drosophila* where R2D2, a cofactor of *Drosophila* Dicer-2, senses the thermodynamic asymmetry of a small interfering RNA (siRNA) duplex and loads the strand

with less-stable 5′ end to Ago2 (Ghildiyal et al., 2010; Liu et al., 2003, 2006; Tomari et al., 2004, 2007). In human, however, it is still debatable whether or not TRBP is required in RISC loading. It has been demonstrated that Dicer and TRBP regulate RISC formation (Noland and Doudna, 2013; Noland et al., 2011). Consistent with this, cells derived from TRBP knockout (KO) mice showed impaired small-hairpin-RNA-mediated silencing activity, suggesting the importance of TRBP in Dicer cleavage and RISC loading (Daniels et al., 2009). In contrast, a recent study indicated that Dicer/TRBP is dispensable in the loading of miRNA onto Ago (Betancur and Tomari, 2012).

Another well-characterized function of TRBP is its role as a cellular inhibitor of dsRNA-dependent protein kinase (PKR) (Park et al., 1994; Sanghvi and Steel, 2011). Upon binding to a stretch of dsRNAs, PKR dimerizes and undergoes autophosphorylation (Patel et al., 1995). Once phosphorylated, PKR suppresses bulk translation by inducing phosphorylation of the α subunit of eIF2 (Meurs et al., 1992) and controls multiple signaling pathways to induce interferon response (Takada et al., 2007; Yang et al., 2010). TRBP forms heterodimer with PKR via dsRBD1 and dsRBD2 in an RNA-independent manner and uses the dsRBD3 to prevent PKR activation (Cosentino et al., 1995; Daher et al., 2001; Gupta et al., 2003). Recently, we have shown that PKR is strongly activated in cells undergoing mitosis (Kim et al., 2014). Yet it is unknown whether the activity of TRBP is modulated in cell cycle and contributes to the mitotic activation of PKR.

In this study, we address the outstanding questions on the function of TRBP by generating transcription-activator-like effector nuclease (TALEN)-based KO HeLa cells. Using these cells, we examined the effect of TRBP depletion on (1) Dicer stabilization, (2) miRNA abundance, (3) Dicer cleavage site selection, and (4) Ago loading. In addition, we also investigated the cell-cycle function of TRBP via its regulation of PKR activation during mitosis. By sequencing small RNAs from the KO cells, we here show that TRBP depletion has no significant effect on overall miRNA abundance but affects Dicer processing of a subset of pre-miRNAs, resulting in the generation of iso-miRs with shifted seed sequences. Similar analysis using PACT and TRBP/PACT double KO cells further confirms that TRBP, but not PACT, regulates the length of mature miRNAs. Moreover, our analysis reveals that TRBP and PACT are dispensable for Ago loading but TRBP can indirectly affect the strand selection because of the shift of cleavage sites. Lastly, we report that TRBP is hyperphosphorylated during mitosis, which augments its inhibitory activity on PKR. Overall, our work provides a comprehensive KO study on the function of human TRBP in miRNA biogenesis and unveils negative feedback regulation of mitotic PKR via hyperphosphorylation of TRBP.

RESULTS

Generation of TRBP KO HeLa Cells

To generate TRBP KO HeLa cells, we used TALEN proteins designed to target human *tarbp2* gene (Figure 1A). In human cells, two adjacent promoters of the *tarbp2* locus produce TRBP1 and TRBP2 mRNA isoforms with TRBP1 mRNA lacking the first exon (Figure 1A; Haase et al., 2005). We therefore designed the TALEN constructs to target a region between dsRBD1 and dsRBD2, which is commonly expressed in both isoforms. Sanger DNA sequencing of genomic DNA extracted from isolated single-cell clones confirmed the presence of frameshift mutations at the target region (Figure S1A). We established cell lines from two of such clones and designated them as TRBP KO no. 1 and no. 2.

We carried out western blotting to confirm the depletion of TRBP protein in these KO clones, which did not show any detectable band around the size of full-length TRBP (Figure 1B). To further confirm the depletion of TRBP, we performed western blot analysis with the lysate from wild-type HeLa cells treated with siRNA against TRBP for 24 hr. Whereas we could still detect weak TRBP band in the knockdown sample, we could not observe any band in the KO samples (Figure S1B). Note that, in both knockdown and KO samples, we did not observe any significant decrease in the level of Dicer, which contradicted the previously reported stabilization effect of TRBP on Dicer (Figures 1B and S1B; Chendrimada et al., 2005). At the same time, our data are consistent with other reports where knockdown of TRBP was not accompanied by decrease in Dicer expression (Haase et al., 2005; Lee et al., 2006). Lastly, we performed a serial dilution of wild-type lysates and estimated the extent of the KO. Whereas we could still detect faint TRBP bands when we loaded 1 μg of protein lysate of wild-type cells, we could not observe any band in 50 μg protein sample of KO cells, indicating that, in our KO cells, TRBP expression is depleted more than 98% of that of the wild-type cells (Figure S1C).

Steady-State Level of miRNAs Remains Unaffected in TRBP KO Cells

Because TRBP is known to interact with Dicer and regulate pre-miRNA processing, we set out to characterize the effect of TRBP KO on the expression level of endogenous miRNAs. We performed deep sequencing for three biological replicates on 18–30 nt RNAs from wild-type and TRBP KO no. 1. Surprisingly, the global distribution of miRNA reads was very similar between wild-type and KO cells, suggesting the abundance of miRNAs might not be affected by TRBP depletion (Figure 1C). Previous studies have identified a subset of miRNAs such as let-7f, miR-99a, and miR-100, whose expression levels were particularly sensitive to the modulation of TRBP (De Vito et al., 2012; Melo et al., 2009). However, even this group of miRNAs did not show any significant change in our high-throughput data (Table S1). Because our analysis cannot rule out the possibility of the global downregulation of miRNAs without affecting their relative distribution, we performed northern blotting and quantitative RT-PCR (qRT-PCR) on a number of miRNAs. In contrast to previous reports, TRBP KO and wild-type cells showed similar miRNA levels (Figures 1D and 1E). Overall, our results suggest that the global pre-miRNA processing is still functional without TRBP and that the steady-state level of miRNAs do not change in cells that lack TRBP.

One possible alternative interpretation of our data is the functional redundancy of TRBP and PACT, another Dicer interactor. PACT is a paralog of TRBP and also consists of three dsRBDs with two N-terminal dsRBDs that are highly similar to those of TRBP dsRBD1 and dsRBD2 (Patel and Sen, 1998). Similar to TRBP, PACT binds near the helicase domain of Dicer via its third

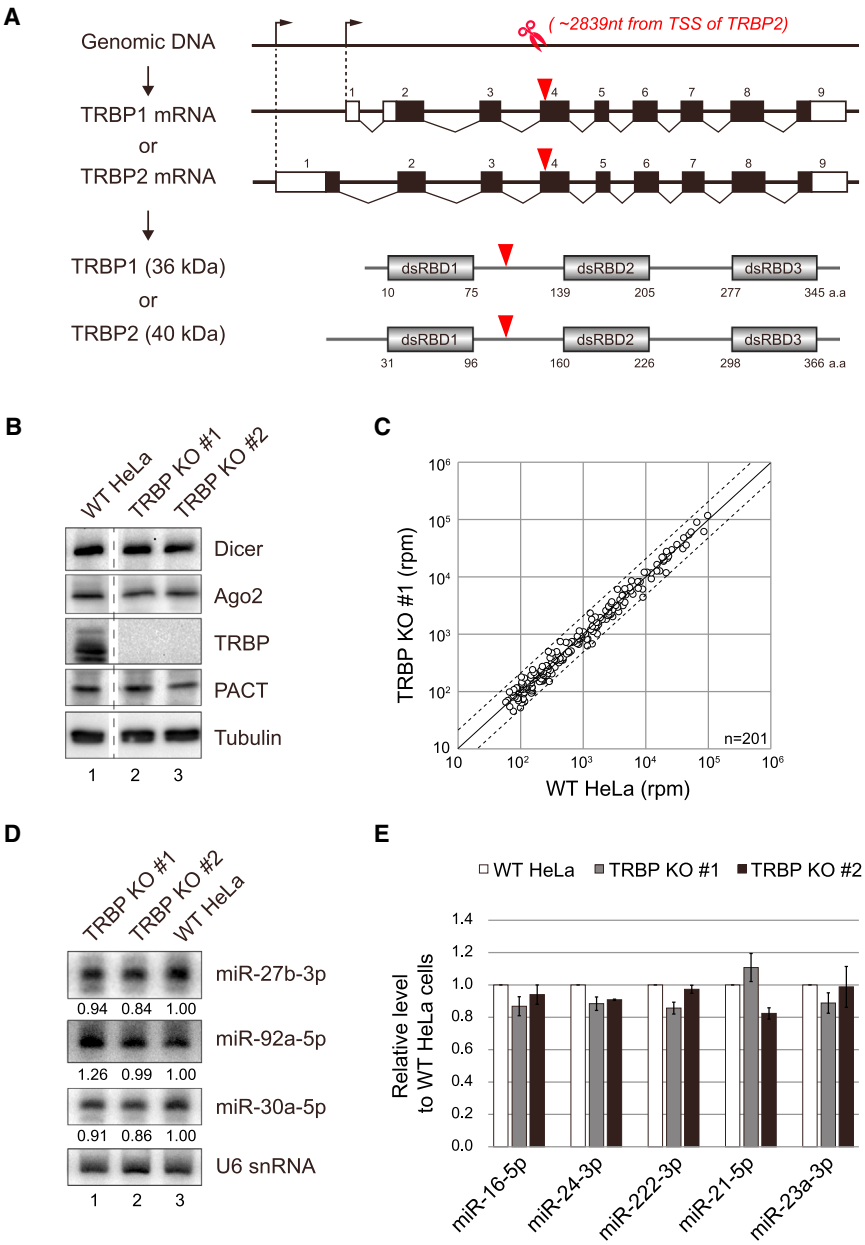

Figure 1. Generation of TRBP KO HeLa Cells with TALEN

(A) Schematics of TRBP mRNA and protein isoforms with scissors indicating the TALEN-targeting region, which is around 2,839 nt downstream of the transcriptional start site (TSS) of TRBP2 mRNA. Red triangles show the corresponding deleted regions in mRNA and protein isoforms.

(B) The depletion of TRBP protein was confirmed by western blotting of KO clones. All lanes are from a single blot, and the excised region is indicated with a dashed line. WT, wild-type.

(C) Small RNA sequencing of TRBP KO and wild-type cells reveal that the global distribution of miRNAs remained unaffected by the depletion of TRBP. An average of three libraries is plotted with dashed lines, indicating the boundaries for 2-fold change. miRNAs with greater than 100 reads per million (rpm) in at least one of the libraries were analyzed.

(D and E) Northern blot analysis (D) and qRT-PCR (E) measurement of several miRNA expressions in the indicated cells. The relative level of each miRNA is normalized first to the intensity of U6 small nuclear RNA and again to the miRNA level from wild-type cells. qRT-PCR data are presented as a mean of three biological replicates with error bars indicating SEM. snRNA, small nuclear RNA.

dsRBD and was proposed to function in pre-miRNA processing based on transient knockdown experiment (Lee et al., 2006). Thus, in TRBP KO cells, PACT may compensate for the loss of TRBP in pre-miRNA processing.

To test this, we generated PACT KO cells using TALEN constructs that target *prkra* gene, which encodes PACT (Figure 2A). In addition, we generated TRBP/PACT double KO cells by transfecting TRBP KO no. 1 with the TALEN plasmids targeting *prkra* loci. We checked the mutation in the targeted region using Sanger DNA sequencing (Figure S1A) and confirmed by western blotting that PACT and/or TRBP expression were successfully abolished in the selected clones (Figure 2B).

Next, we prepared small RNA sequencing libraries with PACT and the double KO cells in order to assess the functional redundancy of TRBP and PACT in Dicer processing. However, similar to our results on TRBP KO cells, the global distribution of miRNAs did not change in PACT KO as well as in the double KO cells (Figure 2C; Table S1). Our subsequent northern blotting and qRT-PCR analysis revealed that the expression levels of selected miRNAs were not affected substantially in these KO cells (Figures 2D and 2E). Overall, our data on various KO cells clearly demonstrate that, at least in HeLa cells, TRBP and PACT do not influence the steady-state level of miRNAs.

TRBP Affects Dicer Cleavage Sites

In addition to affecting the rate, TRBP has been shown to be required for accurate Dicer processing (Fukunaga et al., 2012; Lee and Doudna, 2012). In mouse and fly systems, KO of TRBP or Loqs resulted in the generation of shorter miRNA isoforms, indicating that the accuracy of Dicer cleavage was compromised (Fukunaga et al., 2012). In human, similar shift in Dicer cleavage sites was demonstrated through in vitro reconstitution system using pre-miR-200a (Lee and Doudna, 2012). We explored this miscleavage and generation of iso-miRs globally

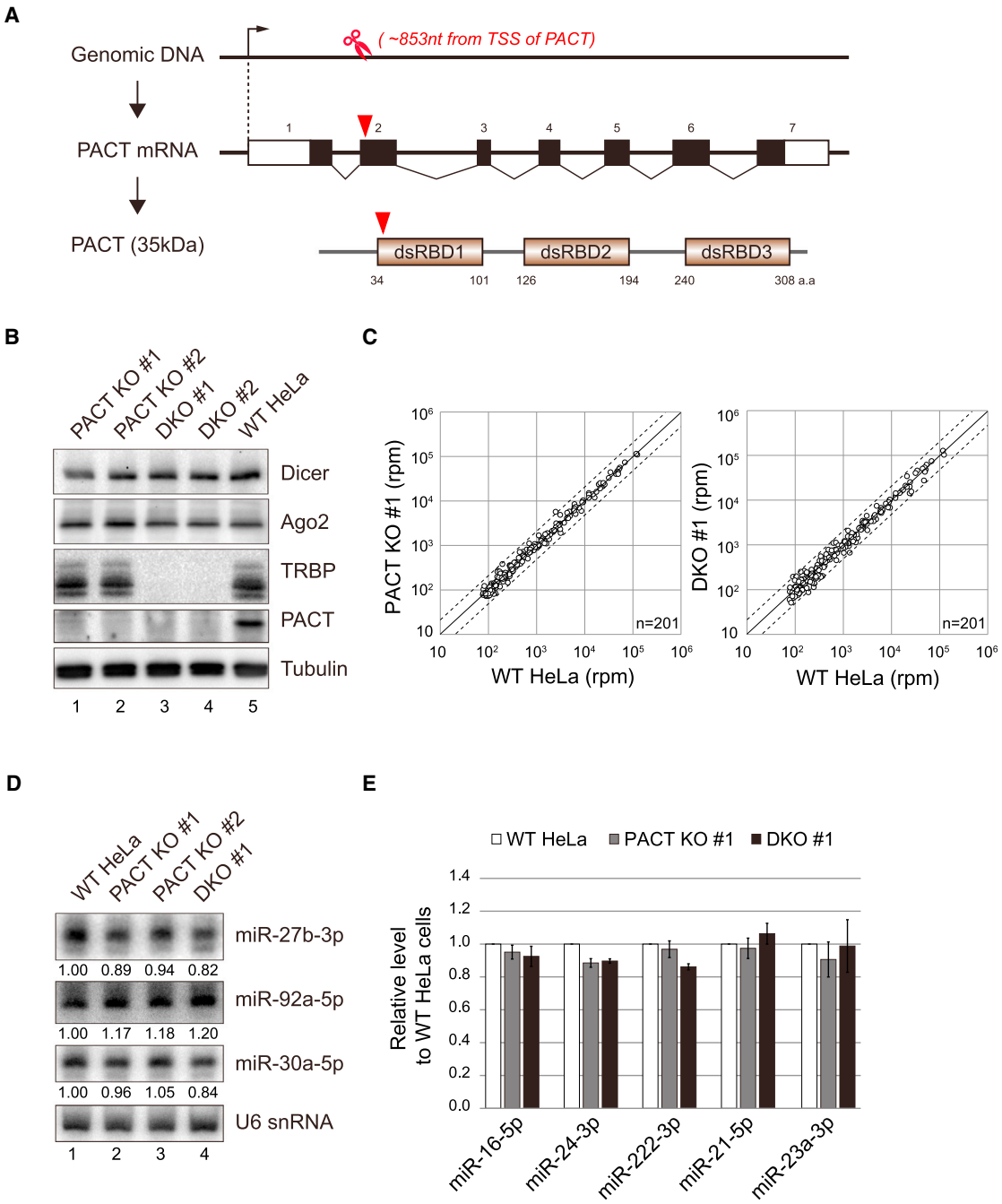

Figure 2. Generation and Characterization of PACT and TRBP/PACT Double KO Cells

(A) A schematic of *prkra* gene with the TALEN target site indicated with scissors. Red triangles denote the location of deletion site in PACT mRNA and protein.

(B) The depletion of PACT and/or TRBP protein was confirmed via western blotting of the KO clones.

(C) Small RNA sequencing revealed that the global distribution of miRNAs remained unaffected by the depletion of PACT and/or TRBP. miRNAs sequencing reads in PACT KO (left) and TRBP/PACT double KO (right) cells are plotted against those of wild-type cells with dashed lines, indicating the boundaries for 2-fold change.

(D and E) Northern blot analysis (D) and qRT-PCR (E) quantification of several miRNA expressions in the indicated cells. The relative level of each miRNA is normalized to that of U6 small nuclear RNA and again to the miRNA level from the wild-type cells. qRT-PCR data are presented as a mean of three biological replicates with error bars indicating SEM.

by analyzing our small RNA sequencing data. As the 3′ ends of miRNAs are frequently modified after Dicer processing (Ameres and Zamore, 2013), we used only the 5′ ends of the 3′-arm-derived miRNAs (3p-miRNAs) to assess Dicer cleavage sites.

To quantify the degree of miscleavage, we first identified the most abundant 3p isoform of a given miRNA in wild-type cells. Then, we examined the change in the expression fraction of this particular isoform (read number of the isoform divided by the sum of all 3p isoforms) between wild-type and TRBP KO cells. We found that, for 13 out of 92 3p-miRNAs examined, this ratio is altered in TRBP KO cells (Figure 3A; Table S2). Note that most of them showed decreased ratio, indicating that the 5′ heterogeneity of 3p-miRNAs is increased (Figure 3A). Our subsequent analysis on PACT and the double KO cells revealed that, whereas similar group of miRNAs showed altered Dicer cleavage sites in the double KO cells, no significant differences were detected in PACT KO cells compared to those of wild-type cells (Figure 3A). Thus, the changes in Dicer cleavage sites we observed in TRBP and the double KO cells likely reflect the effects of TRBP depletion.

As a control, we examined Drosha cleavage sites using the 5′ ends of the 5′-arm-derived miRNAs, which remained unaffected in TRBP KO cells (Figure S2A). Similarly, we detected no significant differences in Drosha-processing sites in PACT and the double KO cells (Figures S2B and S2C). Thus, the observed differences in isoforms are derived from altered Dicer processing, not Drosha processing.

To validate the observed shift in Dicer-processing sites, we carried out northern blot analysis with total RNAs extracted from wild-type and different KO cells. Among the candidate miRNAs tested, miR-126-3p and miR-30a-3p showed an increase in the signal intensity of the band, corresponding to the 1 nt truncated isoform in TRBP and the double KO cells (Figures 3B, 3C, and S3). As a control, we tested the expression patterns of these miRNAs in PACT KO cells, which hardly showed any differences compared to those of wild-type cells (Figures 3B and S3). Considering that the seed sequences of miRNAs are located at 2–7 nt relative to the 5′ ends, our data suggest that, without TRBP, Dicer generates iso-miRs with shifted seed sequences, which would result in the miRNAs targeting a different set of mRNAs (Figure 3C).

TRBP Indirectly Affects Guide Strand Selection

After Dicer cleavage, one strand of the resulting duplex is loaded onto Ago to form RISC. It has been demonstrated using *Drosophila* that the strand selection is determined by the relative thermodynamic stabilities of the base pairs at the 5′ ends of the duplex (Khvorova et al., 2003; Schwarz et al., 2003). For most miRNAs, the strand with the less-stable 5′ end enters the RISC, whereas the other strand undergoes degradation (Schwarz et al., 2003). The observed change in Dicer cleavage sites in TRBP KO cells could potentially reverse the relative thermodynamic stabilities of the duplex, which would alter the strand selection and lead to the loading of the opposite strand onto Ago. Such possibility was already demonstrated by ectopically expressing two different miR-200a duplexes (Lee and Doudna, 2012).

To examine whether this "arm switching" also occurs for endogenous miRNAs, we performed northern blotting on Ago2-immunoprecipitated (IP) RNA from wild-type and different KO cells. First, we checked the IP efficiency by performing western blotting on the immunoprecipitates (Figure S4A). We chose miR-30a as a likely candidate of arm switching based on the thermodynamic stability analysis. Whereas the 5p strand is favored for normal Dicer cleavage products, 3p becomes more favorable strand for truncated miR-30a duplex (Figure S4B). Consistent with our prediction, in TRBP KO cells, Ago2-bound 21 nt miR-30a-3p was accumulated without accompanied increase in the 23 nt 5p strand, which is the complementary strand (Figures 3D and S4C). Similar accumulation of 21 nt 3p strand was observed in our sequencing data, suggesting that more 3p strands become protected by Ago in TRBP KO cells (Figure 3E). Note that this accumulation was not observed in PACT KO cells both in northern blotting and in sequencing data, whereas we observed similar phenomenon in the double KO cells. Therefore, our data provide in cell demonstration of the switch in strand selection by Ago in the absence of TRBP due to Dicer miscleavage.

In all of the KO cells examined, "the thermodynamic stability" rule for the strand selection was still applicable as the strand with less-stable 5′ end entered Ago. This suggests that RISC loading is still functional in the KO cells and TRBP and PACT are dispensable for the guide strand selection. At the same time, our data reveal that TRBP can affect the outcome of strand selection for a number of miRNAs by generating iso-miRs with reversed relative thermodynamic stability.

Combined, our high-throughput analysis of the KO cells reveal that, without TRBP, Dicer exhibits increased frequency of miscleavage of pre-miRNAs that results in truncated iso-miRs with shifted seed sequences and, in some cases, alteration of the strand selection for Ago. At the same time, the steady-state level of miRNAs remained unaffected and Ago loading is still functional. Therefore, we conclude that TRBP is required for accurate processing of a subset of pre-miRNAs by Dicer, but it does not control the rate of Dicer processing and is dispensable for RISC loading.

TRBP Is Hyperphosphorylated during Mitosis

In addition to its role as a Dicer cofactor, TRBP was also implicated as an inhibitor of PKR (Park et al., 1994). Recently, we have shown that PKR is regulated in cell cycle, where it is strongly activated during mitosis by cellular dsRNAs (Kim et al., 2014). PACT, an activator of PKR, did not play a role in the observed activation of PKR (Kim et al., 2014), but the contribution by TRBP remained to be explored. Thus, using TRBP KO cells, we examined possible cell-cycle function of TRBP via its regulation of PKR during mitosis.

We began by testing whether endogenous TRBP can regulate PKR activation. We transfected wild-type and the KO cells with a low dose of polyinosinic:polycytidylic acid (poly I:C), a long dsRNA that can activate PKR (Offermann et al., 1995), and incubated them for 1 hr to mildly induce PKR activation. As a control, we used siLuc duplex that is too short to induce PKR activation. Consistent with previous reports, we found that the degree of PKR activation is greater in TRBP and the double KO cells compared to that of the wild-type cells (Figure 4A; Park et al., 1994; Sanghvi and Steel, 2011). The activity of phospho-PKR (pPKR) assessed by the phosphorylation of eIF2α (peIF2α) was

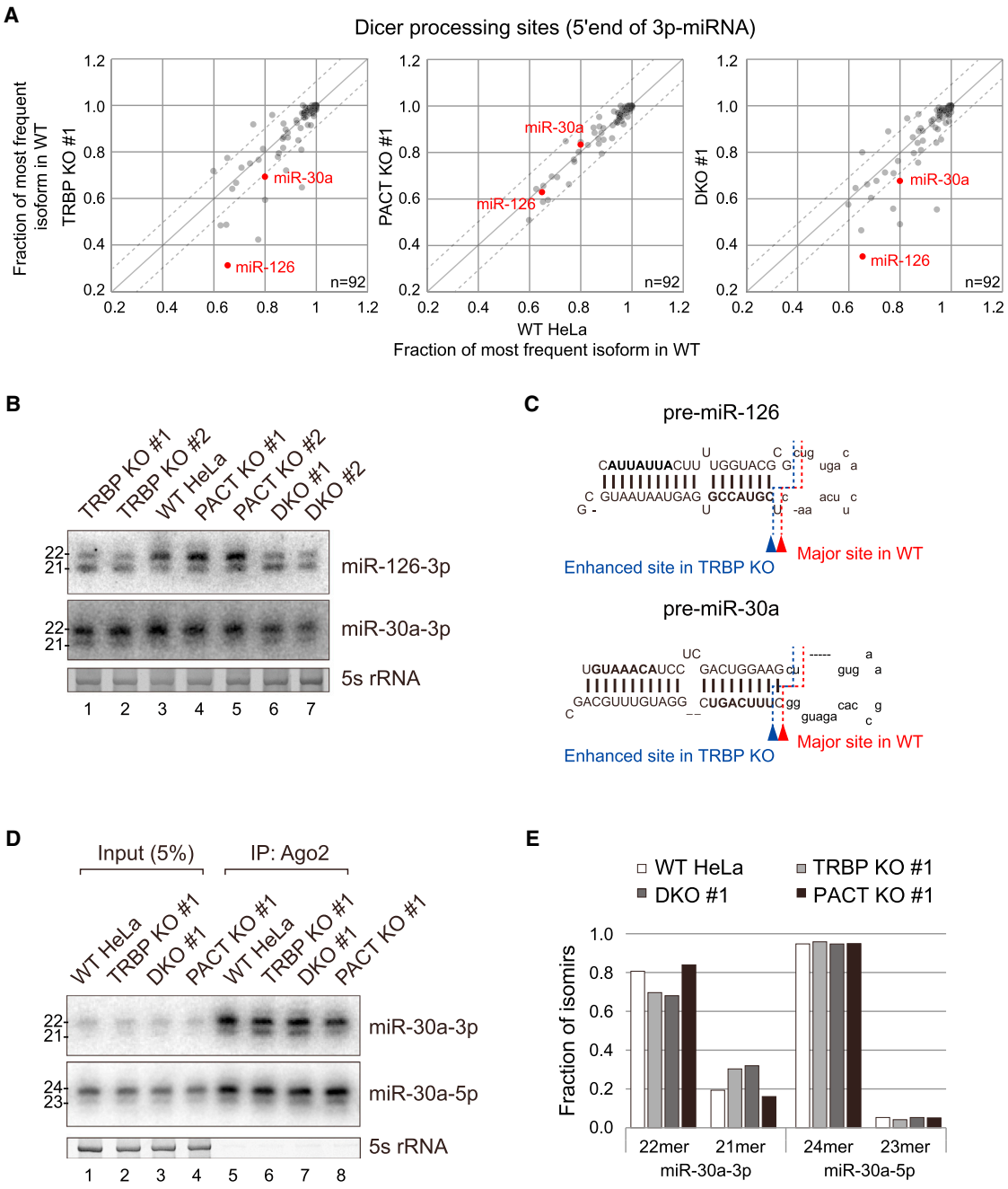

Figure 3. TRBP Depletion Results in Dicer Miscleavage and Arm Switching

(A) The degree of Dicer miscleavage was assessed by identifying the most-abundant isoform of a given 3p miRNA in wild-type cells and comparing how the expression fraction of this particular isoform changes between wild-type and TRBP (left), PACT (middle), or the double KO (right) cells. The red dots represent the miRNAs, whose expression patterns were confirmed via northern blotting.

(B) Northern blotting of miR-126 and miR-30a confirm the generation of truncated iso-miRs in the absence of TRBP whereas they remain unaffected in PACT-depleted cells.

(C) A diagram of pre-miR-126 (upper) and pre-miR-30a (lower) with blue and red dashed lines indicating Dicer cleavage sites in TRBP KO or wild-type cells, respectively. miRNA seed sequences are shown in bold.

(D) Northern blotting of miR-30a on Ago2-IPed RNA show accumulation of 21 nt 3p strand in TRBP KO cells whereas loading of the 5p strand remained unaffected.

(E) Analysis of our sequencing data also confirmed the Ago2-IP result, where we observed increased expression of truncated 3p-strand of miR-30a in the absence of TRBP (TRBP and the double KO) whereas the reads of the corresponding 5p-strand remained unchanged.

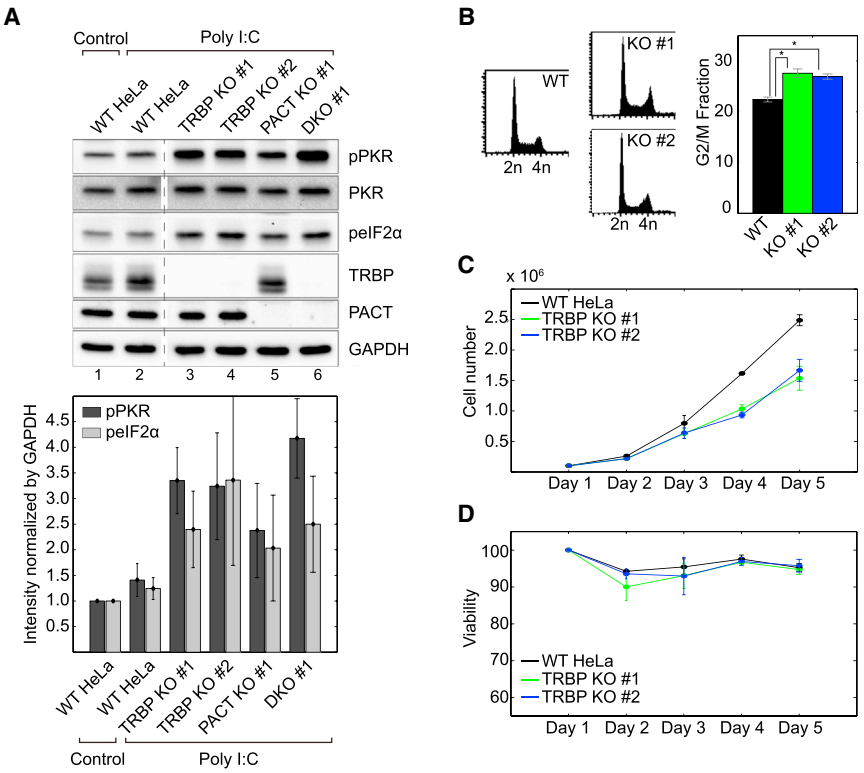

Figure 4. TRBP KO Cells Show Retarded Growth Rate with Prolonged G2/M Phase

(A) Transfection of poly I:C resulted in stronger PKR activation (pPKR) and activity on eIF2α phosphorylation (peIF2α) in TRBP-depleted cells compared to wild-type or PACT KO cells. All lanes are from a single blot, and the excised region is indicated with a dashed line. Quantified band intensity normalized by that of GAPDH is presented below. An average of two biological replicates is shown with SEM as error bars.

(B) FACS profile of wild-type and TRBP KO cells (left), which show increased fraction of cells in G2/M phase. An average of five replicates is shown with error bar indicating SEM (right). *$p < 0.01$.

(C) Growth rate of TRBP KO cells was measured by seeding 100,000 cells and counting the cell number every 24 hr. Both clones show retarded cell growth compared to that of wild-type cells. An average of three replicates is shown with SEM as error bars.

(D) At the same time, the viability was not compromised in the KO cells. An average of three replicates is shown with SEM as error bars.

also increased in TRBP and the double KO cells (Figure 4A). Hence, our data clearly indicate that endogenous TRBP can prevent PKR activation in response to the introduction of long dsRNAs. Of note, depletion of PACT moderately increased the level of pPKR and peIF2α (Figure 4A). One possibility is that PKR activation by PACT requires stress conditions as shown previously (Daher et al., 2009; Singh et al., 2011).

As PKR can regulate cell-cycle progression (Dagon et al., 2001; Kim et al., 2014; Zamanian-Daryoush et al., 1999), we asked whether the depletion of TRBP also affects cell-cycle distribution. Our fluorescence-activated cell sorting (FACS) analysis revealed that TRBP KO cells show increased fraction of cells in G2/M phase (Figure 4B). The magnitude of the effect was mild, but we reproducibly observed similar extent of increase in the fraction of G2/M phase in both KO clones. Increased G2/M fraction is typically accompanied by decrease in G1 fraction, suggesting faster growth. However, we found that the growth rate of the KO clones was slower than that of wild-type cells (Figure 4C). The viability assessed by trypan blue staining was not compromised (Figure 4D), indicating that the decreased growth rate reflects increased duration of the cell cycle rather than increased cell death. Combined with the FACS data, our results indicate that TRBP KO cells show retarded cell growth due to increased duration of G2/M phase. As overexpressing PKR in Chinese hamster ovary cells resulted in G2/M phase arrest (Dagon et al., 2001), the observed increase in G2/M population is consistent with overactivation of PKR in TRBP KO cells.

To examine possible cell-cycle-dependent regulation of TRBP, we performed western blotting on wild-type asynchronous (AS) cells or cells arrested in G1, S, or M phase (see Experimental Procedures for details). Interestingly, we observed a mobility shift of TRBP by ~5 kDa in M-phase-arrested cells (Figure 5A). To test if this slow migrating band reflected modified form of the protein, we arrested TRBP KO no. 1 in S or M phase following the same arrest scheme as we used for wild-type cells. We could not detect any TRBP bands in the KO cells, suggesting that our antibody is specifically detecting TRBP protein in both phases, and the slowly migrating band is indeed a modified form of TRBP (Figure S5). Thus, we conclude that TRBP is posttranslationally modified in M phase, which results in the mobility shift of the protein on a SDS-PAGE gel.

To rule out the possibility that the observed phenomenon was an artifact of nocodazole treatment, we monitored TRBP expression in cells released from the double thymidine block, which synchronized cells at S phase. Using FACS, we confirmed that the cells progress through cell cycle in near synchrony (Figure 5B, lower panel). The slow-moving TRBP band appeared ~8 hr after the release as cells began to enter M phase (Figure 5B). The maximum level of the modified TRBP expression occurred 2 hr later, when most of the cells exited the mitotic phase. Note that the modified TRBP was detected again 22 hr after the release, when the cells entered M phase for the second time (Figure 5B). Thus, our data suggest that TRBP is reversibly modified in M phase of proliferating cells.

Considering that a large number of proteins are phosphorylated in M phase (Olsen et al., 2010) and phosphorylation could lead to retardation of protein mobility on a SDS-PAGE gel, we examined whether TRBP was phosphorylated. We prepared total protein lysates of AS cells or cells arrested in S or M phase and treated them with λ phosphatase for 30 min at 30°C. The modified TRBP band was nearly completely abolished, and the

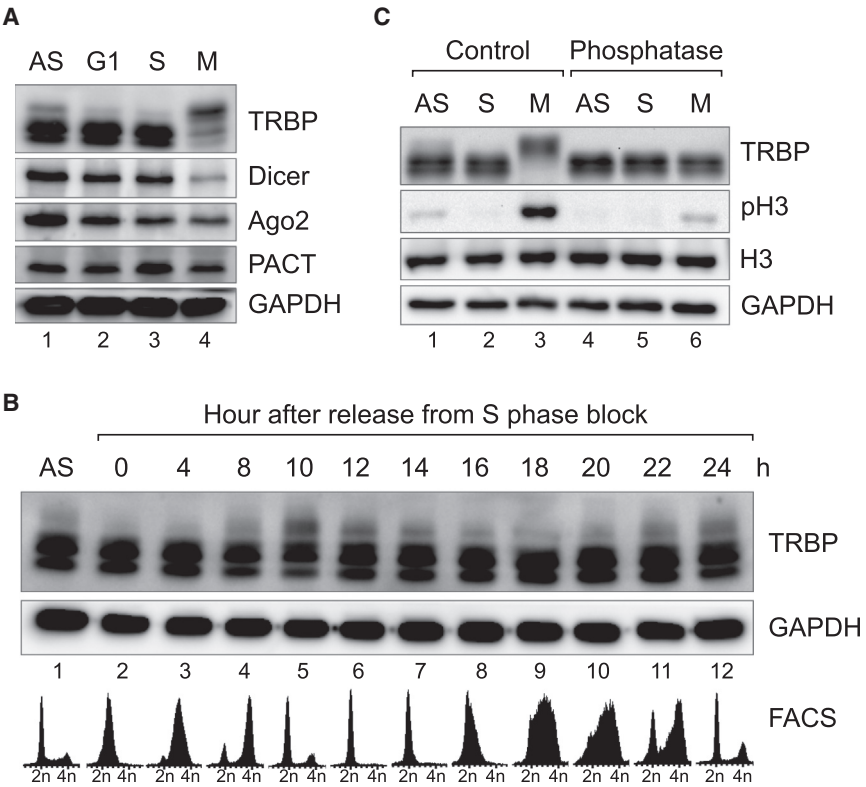

Figure 5. TRBP Is Hyperphosphorylated during Mitosis

(A) Western blot of TRBP, Dicer, Ago2, and PACT in HeLa cells arrested at different cell-cycle phases. A slowly migrating band corresponding to modified TRBP is observed in M-phase-arrested sample.

(B) Dynamic pattern of TRBP modification in cell cycle was examined by releasing cells synchronized at S phase and collecting them every 2–4 hr.

(C) Treating the total cell lysate of M-phase-arrested cells with λ phosphatase resulted in the increased mobility of TRBP on a SDS-PAGE gel. Phospho-histone H3 (pH3), which specifically appears during mitosis, was used as a positive control of the phosphatase treatment.

unmodified band was restored by the phosphatase treatment (Figure 5C). We denote our observation as "hyperphosphorylation" of TRBP to distinguish it from a previously reported phosphorylation by ERK (Paroo et al., 2009).

JNK Is an Upstream Kinase of TRBP Hyperphosphorylation

Next, we sought out the upstream signal of TRBP hyperphosphorylation by using small chemical inhibitors of different signaling pathways. We treated M-phase-arrested cells with the following inhibitors: Ly294002 phosphatidylinositol 3-kinase inhibitor; rapamycin mTOR inhibitor; GF109203X PKC inhibitor; PD98059 MEK inhibitor; SP600125 JNK inhibitor; and SB203580 p38 mitogen-activated protein kinase inhibitor. Notably, MEK inhibitor treatment had no effect, suggesting that TRBP hyperphosphorylation is clearly different from previously reported TRBP phosphorylation by ERK (Figure 6A; Paroo et al., 2009). Instead, we observed clear dephosphorylation of TRBP when we treated cells with SP600125 for 3 hr, indicating that TRBP is phosphorylated by JNK or by its downstream kinase (Figure 6A).

To test whether JNK can directly phosphorylate TRBP, we performed in vitro kinase assay using purified JNK and TRBP. Because we and others have shown that JNK is activated during mitosis (Kim et al., 2014; Ribas et al., 2012), we purified phospho-JNK (pJNK) from M-phase-arrested cells and incubated it with full-length recombinant TRBP (glutathione S-transferase [GST]-TRBP) and radioisotope-labeled ATP. We observed a distinct band of autoradiography signal at a size corresponding to GST-TRBP (Figure 6B). As a control, we incubated purified pJNK with just GST, which did not show any specific autoradiography signal (Figure 6B). Thus, our in vitro kinase assay clearly indicates that TRBP is directly phosphorylated by pJNK purified from mitotic cells, although we cannot exclude a possibility that other kinases may also participate in TRBP phosphorylation in cells.

We further characterized TRBP hyperphosphorylation by identifying putative phosphorylation sites. We used NetPhos 2.0 software (Blom et al., 1999) and obtained a total of 12 serine and threonine residues that are likely to be phosphorylated by pJNK. We then generated three different phospho mutant constructs of TRBP (Figure 6C): one with all 12 sites mutated to alanine (TRBP-mut 1); one with the N-terminal eight sites mutated (TRBP-mut 2); and one with the C-terminal four sites mutated (TRBP-mut 3). When we ectopically expressed these TRBP mutant constructs in M-phase-arrested cells, the first two failed to be phosphorylated whereas the last one showed a pattern similar to that of wild-type TRBP (Figure 6D). Note that ectopic expression of wild-type and TRBP-mut 3 resulted in a significant fraction of the protein remained as unmodified. This is likely due to very high expression level of exogenous TRBP, which overwhelmed the amount of its modifying enzyme. Hence, we conclude that N-terminal region of TRBP is phosphorylated during mitosis.

TRBP Hyperphosphorylation Is a Widespread Phenomenon Occurring during Mitosis

Considering that cell cycle is a general process, we hypothesized that TRBP hyperphosphorylation occurs in other cells derived from different tissues. Previously, we have shown that JNK is phosphorylated in multiple cancer cells as well as in mouse embryonic stem cells during mitosis (Figures 6E–6G; Kim et al., 2014). We also observed hyperphosphorylation of TRBP in these cells (Figures 6E–6G). Hence, hyperphosphorylation is a common feature occurring across multiple cancer cell lines (cervical: HeLa, leukemia: K562, and breast: MDA-MB-231) as well as in non-cancer, nonhuman cell line (mouse embryonic stem cells: R1).

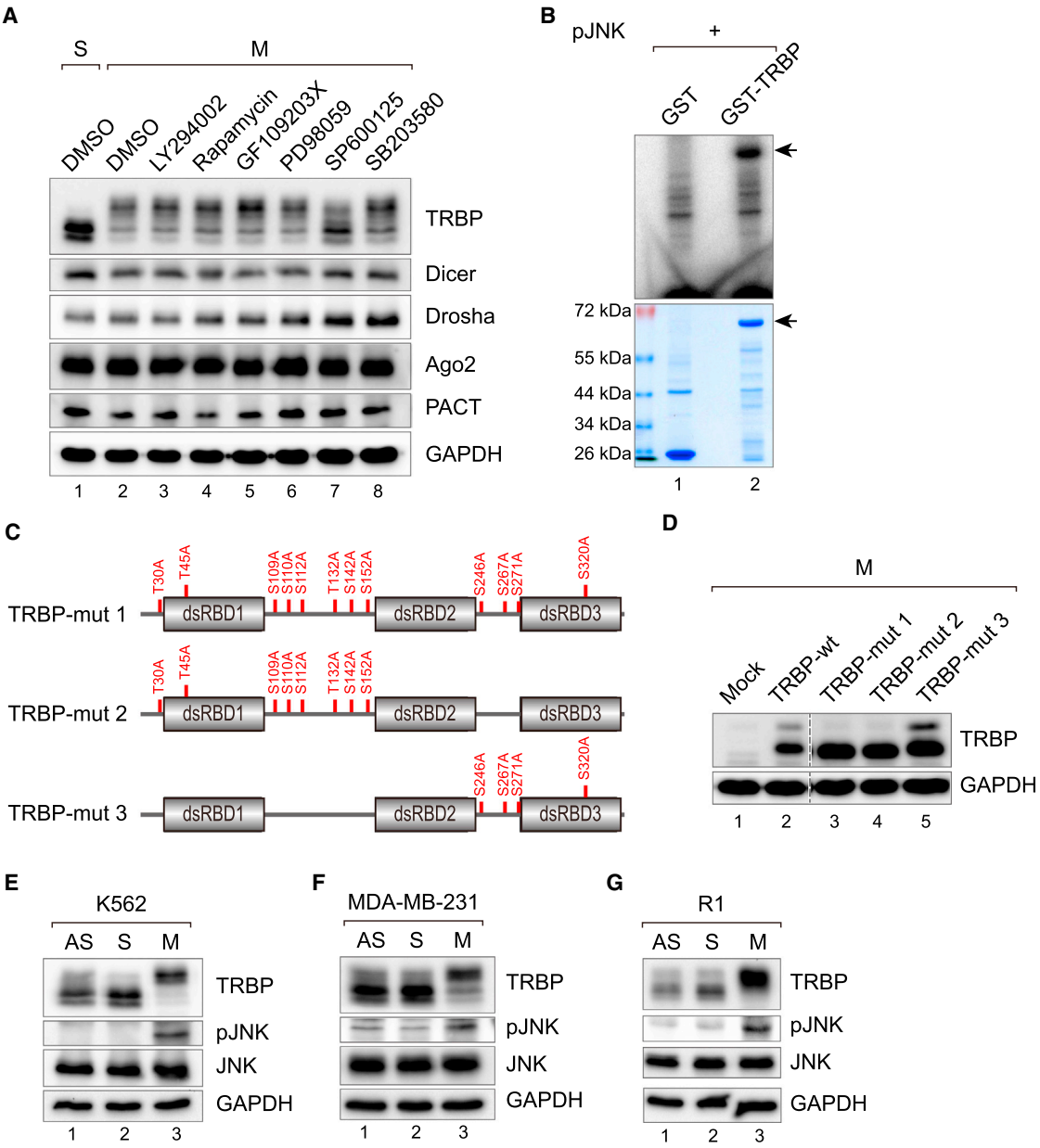

Figure 6. JNK Is an Upstream Kinase of TRBP Hyperphosphorylation

(A) Western blot of M-phase-arrested cells treated with different kinase inhibitors. TRBP is dephosphorylated when cells were treated with the JNK inhibitor SP600125.

(B) Incubation of GST-TRBP with pJNK immunoprecipitated from M-phase-arrested cells resulted in the phosphorylation of TRBP, indicated by the strong autoradiography signal at the region corresponding to GST-TRBP. Autoradiography is shown on the top with Coomassie staining on the bottom. Arrows indicate the location of GST-TRBP.

(C) Schematics of the three TRBP phospho mutant constructs used in this study.

(D) Ectopic expression of TRBP mutant constructs in M-phase-arrested cells revealed that the putative phosphorylation sites are located in the N-terminal region of the protein, as TRBP-mut 1 and -mut 2 were not phosphorylated. All lanes are from a single blot, and the excised region is indicated with a dashed line.

(E–G) Western blotting of cell-cycle-arrested K562 (E), MDA-MB-231 (F), or R1 (G) cells showed that the mitotic activation of JNK and hyperphosphorylation of TRBP occur in multiple cell lines.

Hyperphosphorylation Enhances Inhibitory Activity of TRBP on PKR

To understand the biological function of TRBP hyperphosphorylation, we first examined whether the subcellular localization was affected. However, our immunocytochemistry data showed that TRBP remained dispersed throughout the cytosol in both S- and M-phase-arrested cells (Figure 7A). We then performed coIP and examined the interaction between TRBP with its known binding

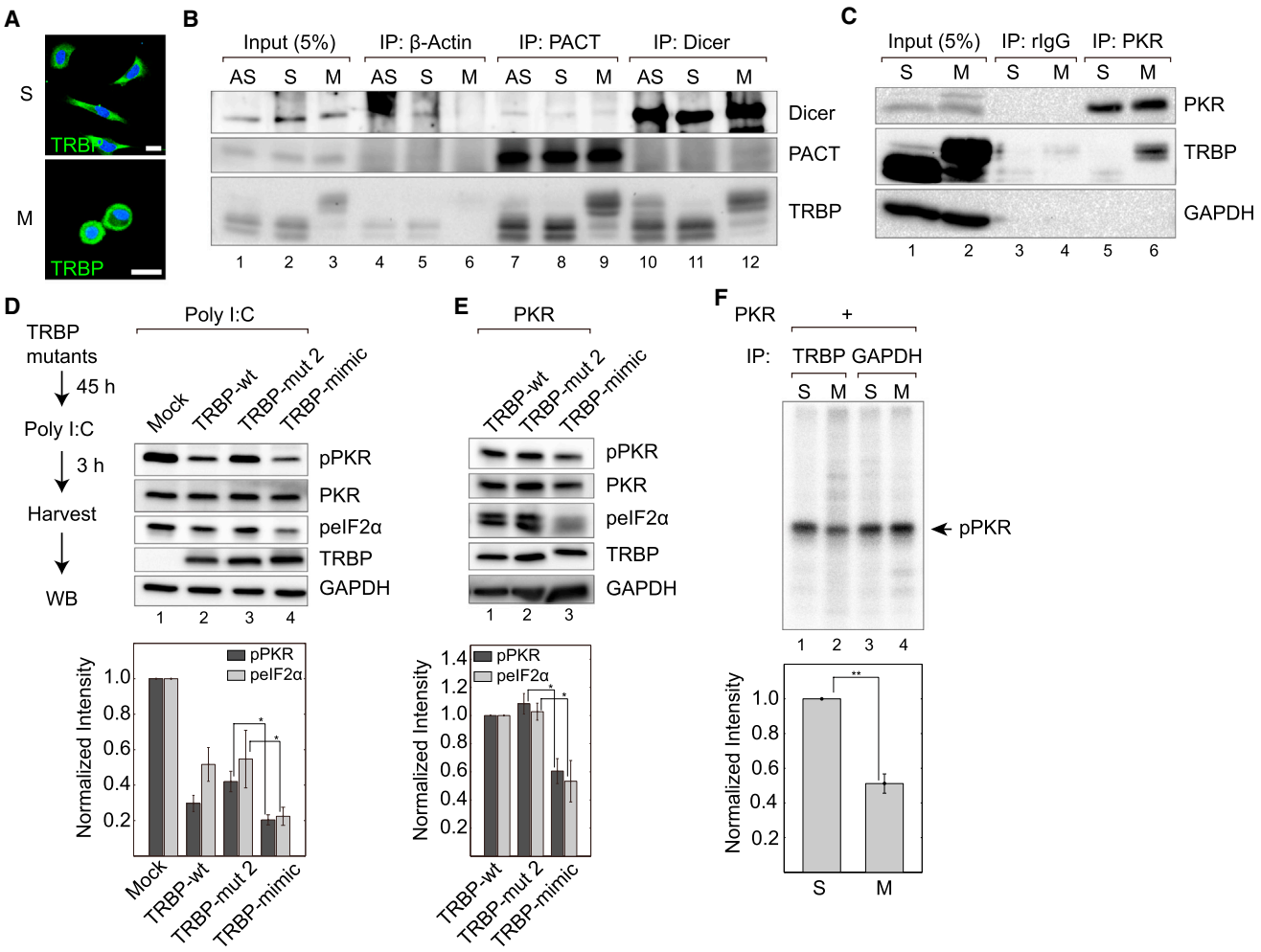

Figure 7. Hyperphosphorylation Enhances the Inhibitory Activity of TRBP on PKR

(A) Immunocytochemistry of TRBP in S- or M-phase-arrested cells. TRBP is distributed throughout the cytosol in both phases.

(B) Immunoprecipitating Dicer or PACT in AS-, S-, or M-phase-arrested cells reveal that the amount of TRBP bound to Dicer or PACT stayed nearly constant in cell cycle.

(C) At the same time, immunoprecipitating PKR resulted in more TRBP coIPed in M-phase-arrested sample. IgG, immunoglobulin G.

(D) Induction of PKR activation by transfecting poly I:C on cells expressing different TRBP constructs. Western blotting analysis reveal that the phospho-mimic TRBP showed the strongest effect on suppressing PKR activation and its activity on phosphorylating eIF2α. Quantified western blot signal intensity for pPKR and peIF2α normalized by that of GAPDH is presented below. An average of three biological replicates is shown with error bars representing SEM. *$p < 0.05$. WB, western blot.

(E) Similarly, coexpression of PKR with different TRBP constructs also resulted in the phospho-mimic TRBP showing the strongest inhibitory activity on PKR activation and activity. Quantified western blot signal intensity for pPKR and peIF2α normalized by that of GAPDH is presented below. An average of three biological replicates is shown with error bars representing SEM. *$p < 0.05$.

(F) In vitro PKR phosphorylation assay confirms that pTRBP immunoprecipitated from M-phase-arrested cells is more effective in suppressing PKR autophosphorylation compared to unphosphorylated TRBP from S-phase-arrested cells. GAPDH immunoprecipitate was used as a negative control. Location of pPKR is indicated with an arrow. The relative autoradiography signal of pPKR for samples incubated with TRBP immunoprecipitates is presented below. An average of four biological replicates is shown with error bars representing SEM. **$p < 0.01$.

partners, specifically Dicer, PACT, and PKR. When we pulled down Dicer or PACT, we did not observe any significant differences between cell cycle samples, suggesting that TRBP hyperphosphorylation does not affect its interaction with Dicer or PACT (Figure 7B). At the same time, when we pulled down PKR, we observed a significant increase in the amount of TRBP coIPed in M-phase-arrested cells compared to those in S-phase-arrested cells (Figure 7C). The coIP results indicate that the interaction between TRBP and PKR is enhanced when TRBP is hyperphosphorylated.

The dominant action mechanism of TRBP-mediated inhibition of PKR is via direct binding (Cosentino et al., 1995; Gupta et al., 2003). Thus, we asked whether the increased interaction between TRBP and PKR can strengthen the activity of TRBP

on inhibiting PKR. First, we generated a phospho-mimic form of TRBP (TRBP-mimic) by replacing eight putative phosphorylation sites of TRBP to aspartic acid. We then expressed phospho mutant 2 or phospho-mimic form of TRBP on TRBP KO cells and performed PKR IP experiment. We found that phospho-mimic TRBP interacted more strongly to PKR than the phospho mutant (Figure S6A). This is consistent with our earlier IP experiment using cell cycle samples, where hyperphosphorylated TRBP showed increased interaction with PKR (Figure 7C). To further confirm our data, we performed a converse IP experiment where we pulled down TRBP using flag beads and examined the amount of coIPed PKR. We again observed that phospho-mimic TRBP interacted more strongly to PKR than the phospho mutant (Figure S6B). Of note, the increased interaction between PKR and phospho-mimic TRBP occurred only when we transfected cells with poly I:C to induce PKR activation. This suggests that pTRBP may interact more strongly to pPKR than to PKR.

To test the effect of increased interaction between TRBP and PKR, we examined the ability of different TRBP mutants in inhibiting PKR. We first expressed wild-type, phospho mutant 2, or phospho-mimic TRBP on TRBP KO no. 1. Approximately 45 hr later, we transfected these cells with poly I:C and incubated them for additional 3 hr to induce PKR activation. We observed reduced PKR activation in cells with ectopic TRBP expression compared to Mock control cells that were transfected with a null vector (Figure 7D). This result again confirms that TRBP is indeed an inhibitor of PKR. More importantly, this inhibitory effect of TRBP on PKR is augmented when the phospho-mimic form was expressed (Figure 7D). This effect is also apparent when we examined the pattern of peIF2α, which can be used as readout of pPKR activity (Figure 7D). The amount of TRBP expressed is similar in all three samples, suggesting that phospho-mimic TRBP is a more-potent inhibitor of PKR, which is likely due to its stronger interaction to PKR.

An alternative way of activating PKR is by simply overexpressing the protein. Hence, we cotransfected cells with plasmids expressing *flag-PKR* and one of the three TRBP proteins for 48 hr. We observed a significant cell death when PKR was overexpressed with a blank vector (Mock sample) and could not include it in this analysis. By just comparing other three samples that coexpress PKR and different forms of TRBP, we found that phospho-mimic TRBP showed the strongest inhibitory effect on PKR activation as well as on its activity to phosphorylate eIF2α (Figure 7E).

Lastly, we tested the effect of pTRBP on PKR more directly by performing in vitro kinase assay. We utilized the fact that the upstream kinase of PKR activation is another PKR molecule, and thus, we did not need purified activator of PKR. We combined purified PKR with TRBP immunoprecipitated from S- or M-phase-arrested cells and examined the activation of PKR by measuring the incorporation of radioisotope-labeled ATP. We found that, when PKR is incubated with TRBP from M-phase-arrested cells, the level of pPKR visualized by autoradiography signal was reduced (Figure 7F). As a control, we used immunoprecipitated GAPDH to rule out the possibility that the observed effect was due to a small amount of phosphatase present in the immunoprecipitate from M-phase-arrested cells. Together, these evidences suggest that hyperphosphorylation enhances the inhibitory activity of TRBP on PKR.

DISCUSSION

TRBP is a ubiquitously expressed protein that mediates cross-talk between different cellular processes (Daniels and Gatignol, 2012). It is implicated in the regulation of miRNA biogenesis as well as in the inhibition of PKR (Haase et al., 2005; Park et al., 1994). In this study, we generated TALEN-based TRBP KO HeLa cells to evaluate the two cellular functions of TRBP. With regard to its controversial role in Dicer stabilization, our data show that TRBP does not stabilize the protein. In addition, TRBP does not regulate the steady-state level of miRNAs but is required for accurate processing of a subset of miRNAs such as miR-30a and miR-126. This is consistent with the previous in vitro study where processing by recombinant Dicer alone led to increased production of iso-miRs (Lee and Doudna, 2012). Furthermore, we demonstrate that TRBP is dispensable for Ago loading of Dicer cleavage products but can affect the strand selection indirectly by changing Dicer-processing sites. Lastly, we also generate cells lacking PACT and TRBP/PACT double KO cells to compare TRBP and PACT as Dicer interactors in pre-miRNA processing. Our data indicate that two proteins do not functionally compensate for one another and that PACT does not play a role in miRNA biogenesis at least in HeLa cells.

Previously, we have reported that PACT binds to Dicer based on overexpression experiments and that PACT regulates pre-miRNA processing based on transient RNAi experiment (Lee et al., 2006). In contrast to this, PACT KO did not have any significant effects on either Dicer processing or miRNA abundance. One possible explanation is that the previous report used overexpression system. Under such condition, we observed strong interaction between PACT and Dicer that was comparable to the one between TRBP and Dicer (Lee et al., 2006). However, this was certainly not the case in HeLa cells where endogenous Dicer bound more strongly to TRBP than to PACT (Figure 7B). Thus, it is possible that, although PACT has the potential to regulate pre-miRNA processing, its endogenous interaction to Dicer is too weak that the depletion of PACT had no effect on the expression patterns of miRNAs. Perhaps there exist certain stress conditions or tissue types in which PACT shows increased binding to Dicer and contributes to pre-miRNA processing. The role of PACT in miRNA biogenesis requires further investigation in the future.

Our study shows that TRBP depletion has differential miRNA-specific effects. Previous efforts on analyzing pre-miRNA processing have proposed a number of rules on substrate recognition and cleavage by Dicer (Heo et al., 2012; Park et al., 2011; Zhang et al., 2004), but they fail to provide an explanation for our observation. Furthermore, it is unknown why Dicer cleavage sites are shifted by 1 nt in TRBP or the double KO cells. Perhaps binding to TRBP alters the conformation of Dicer protein and helps it to accurately measure 22 nt from the ends of pre-miRNAs. More likely, TRBP may change the conformation of the pre-miRNA bound to Dicer. Structural studies on Dicer-TRBP complex will provide an explanation on the observed role of TRBP and enhance our understanding of pre-miRNA processing by the complex.

Among the miRNAs with shifted Dicer-cleavage sites, miR-126 showed the most dramatic change, where the appearance of the

21 nt iso-miR was clearly detectable by northern blotting. This truncation at the 5′ end would alter the seed sequences of the miRNA and thereby change its target pools. Unfortunately, this miRNA is expressed in low abundance in HeLa cells, and consequently, generation of its iso-miRs had negligible effects on target derepression (data not shown). Considering the tissue specificity in miRNA expression, our results suggest that TRBP might have tissue-specific roles. Consistent with this, it has been shown that TRBP KO mice showed the most pronounced defects in spermatogenesis (Zhong et al., 1999). Based on our data, TRBP-sensitive miRNAs might be expressed at high levels and play a role in developing germ cells. In addition, given that the expression of TRBP is quite variable among different cell lines, it is possible that animals might be utilizing this variation in TRBP levels to generate iso-miRs in a tissue-specific manner. It will be interesting to compare the effect of TRBP depletion in multiple tissues with different miRNA- and TRBP-expression profiles.

By analyzing TRBP KO cells, we discovered cell-cycle-dependent posttranslational modification of TRBP. Phosphorylation of TRBP has been reported previously, where ERK phosphorylates TRBP at four residues, which strengthens its interaction with Dicer and affects the expression of miRNAs (Paroo et al., 2009). We found that TRBP undergoes hyperphosphorylation during mitosis by pJNK and that pTRBP shows increased binding to PKR. Consequently, hyperphosphorylation enhances the inhibitory activity of TRBP on PKR.

When activated, PKR can regulate multiple signaling pathways, one of which being JNK (Takada et al., 2007). We have recently shown that the mitotic expression of pJNK requires PKR activation (Kim et al., 2014). Together, our data suggest a negative feedback control of PKR activation during mitosis, where PKR is modulating its own activation status by regulating its inhibitor TRBP via JNK. In addition, the observed feedback regulation of PKR is likely to be present in cells derived from different tissues, as we observed the phosphorylation of the components of the feedback module in multiple cell lines (Kim et al., 2014). Nevertheless, the importance of this feedback regulation in cell division remains to be tested. One possibility is the fine tuning of PKR activation level, which might be important in preventing cell death during mitosis. Considering that cells of different heritage respond differently to prolonged mitotic arrest (Topham and Taylor, 2013), this type of regulation might be particularly important in the survival of the cells that are more prone to death during mitosis.

Although JNK is necessary, it is unknown whether JNK activation is also a sufficient condition for TRBP hyperphosphorylation. Considering that the downstream effect of TRBP hyperphosphorylation is modulation of PKR activation, it is possible that both PKR and JNK must be activated to induce TRBP hyperphosphorylation. At the same time, there may exist additional mitosis-specific kinase of TRBP. In the future, analysis of its upstream kinases will be required for better understanding of TRBP hyperphosphorylation and the role of TRBP in cell-cycle progression.

EXPERIMENTAL PROCEDURES

Generation of TALEN Constructs

TALEN constructs used in this study were composed of TALE repeat domains and a FokI nuclease domain. They were designed to target the open reading frame region of *tarbp2* or *prkra* gene (Table S3). TALENs were synthesized by ToolGen as described previously (Kim et al., 2013a, 2013b).

Generation of KO Cell Lines

The TALEN and reporter plasmids were transfected into HeLa cells with Lipofectamine 2000 (Life Technologies) following the manufacturer's instruction. For enrichment of KO cells, the surrogate reporters were constructed as described previously (Kim et al., 2013c). Forty-eight hours after the transfection, H-2K^k-positive cells were separated with a magnetic-activated cell-sorting system (Miltenyi Biotec) according to the manufacturer's instructions. The separated cells were plated at a density of 100∼500 cells per 100 mm dish and were incubated until colony formation. After single-cell cloning, T7 endonuclease I assays were carried out to detect DNA mutation. Success of the target deletion in the KO cell lines was confirmed by fluorescent PCR, Sanger DNA sequencing, and expression analysis via western blotting.

Deep Sequencing of Small RNAs

Small RNA libraries were prepared using TruSeq small RNA sample preparation kit (Illumina). Total RNA was extracted using TRIzol reagent (Life Technologies), and 10 μg was then separated on 15% urea-PAGE. A region corresponding to ∼18–30 nt was gel-purified and ligated to 3′ adaptor with T4 RNA ligase2 truncated (New England Biolabs). After gel purification of the 3′-adaptor-ligated RNA, 5′ adaptor was ligated using T4 RNA ligase1. Adaptor-ligated small RNAs were then reverse transcribed using SuperScript II (Life Technologies), amplified by PCR with Phusion DNA polymerase, and sequenced by Illumina Miseq.

Analysis of Deep Sequencing

The workflow for the sequencing analysis was as previously described (Park et al., 2011). For analysis of cleavage site change, we first selected reads that perfectly match to miRBase mature miRNA and calculated the fraction of 3p or 5p strand isoforms whose lengths vary by one or more nt at the 5′ end (5′ isoform). Changes of the cleavage sites were assessed by comparing the expression fraction of the most-frequent 5′ isoform of 3p or 5p miRNAs of wild-type cells to that of KO cells.

ACCESSION NUMBERS

High-throughput sequencing data have been deposited in the NCBI Gene Expression Omnibus database with accession number GSE61458.

SUPPLEMENTAL INFORMATION

Supplemental Information includes Supplemental Experimental Procedures, six figures, and three tables and can be found with this article online at http://dx.doi.org/10.1016/j.celrep.2014.09.039.

AUTHOR CONTRIBUTIONS

Y.K., J.Y., J.H.L., and V.N.K. designed the project. Y.K., J.Y., J.H.L., J.C., and J.-S.K. performed experiments. All authors analyzed the data. J.Y. and D.S. carried out bioinformatics analysis. Y.K., J.Y., J.H.L., and V.N.K. wrote the manuscript.

ACKNOWLEDGMENTS

We thank Dr. Mourelatos Zissimos for providing the Ago2 antibody. We are also grateful for Dr. Young-Kook Kim and Yeon Choi for their help with generation and analysis of sequencing data. We thank Sun Ah Kim for technical support and appreciate other members of our laboratory for their helpful discussions. This research was supported by IBS-R008-D1 of the Institute for Basic Science and the TJ Park Postdoctoral Fellowship (to Y.K.).

Received: August 22, 2014
Revised: September 12, 2014
Accepted: September 22, 2014
Published: October 23, 2014

REFERENCES

Ameres, S.L., and Zamore, P.D. (2013). Diversifying microRNA sequence and function. Nat. Rev. Mol. Cell Biol. *14*, 475–488.

Bernstein, E., Caudy, A.A., Hammond, S.M., and Hannon, G.J. (2001). Role for a bidentate ribonuclease in the initiation step of RNA interference. Nature *409*, 363–366.

Betancur, J.G., and Tomari, Y. (2012). Dicer is dispensable for asymmetric RISC loading in mammals. RNA *18*, 24–30.

Blom, N., Gammeltoft, S., and Brunak, S. (1999). Sequence and structure-based prediction of eukaryotic protein phosphorylation sites. J. Mol. Biol. *294*, 1351–1362.

Chendrimada, T.P., Gregory, R.I., Kumaraswamy, E., Norman, J., Cooch, N., Nishikura, K., and Shiekhattar, R. (2005). TRBP recruits the Dicer complex to Ago2 for microRNA processing and gene silencing. Nature *436*, 740–744.

Cosentino, G.P., Venkatesan, S., Serluca, F.C., Green, S.R., Mathews, M.B., and Sonenberg, N. (1995). Double-stranded-RNA-dependent protein kinase and TAR RNA-binding protein form homo- and heterodimers in vivo. Proc. Natl. Acad. Sci. USA *92*, 9445–9449.

Dagon, Y., Dovrat, S., Vilchik, S., Hacohen, D., Shlomo, G., Sredni, B., Salzberg, S., and Nir, U. (2001). Double-stranded RNA-dependent protein kinase, PKR, down-regulates CDC2/cyclin B1 and induces apoptosis in non-transformed but not in v-mos transformed cells. Oncogene *20*, 8045–8056.

Daher, A., Longuet, M., Dorin, D., Bois, F., Segeral, E., Bannwarth, S., Battisti, P.L., Purcell, D.F., Benarous, R., Vaquero, C., et al. (2001). Two dimerization domains in the trans-activation response RNA-binding protein (TRBP) individually reverse the protein kinase R inhibition of HIV-1 long terminal repeat expression. J. Biol. Chem. *276*, 33899–33905.

Daher, A., Laraki, G., Singh, M., Melendez-Peña, C.E., Bannwarth, S., Peters, A.H., Meurs, E.F., Braun, R.E., Patel, R.C., and Gatignol, A. (2009). TRBP control of PACT-induced phosphorylation of protein kinase R is reversed by stress. Mol. Cell. Biol. *29*, 254–265.

Daniels, S.M., and Gatignol, A. (2012). The multiple functions of TRBP, at the hub of cell responses to viruses, stress, and cancer. Microbiol. Mol. Biol. Rev. *76*, 652–666.

Daniels, S.M., Melendez-Peña, C.E., Scarborough, R.J., Daher, A., Christensen, H.S., El Far, M., Purcell, D.F., Lainé, S., and Gatignol, A. (2009). Characterization of the TRBP domain required for dicer interaction and function in RNA interference. BMC Mol. Biol. *10*, 38.

Daviet, L., Erard, M., Dorin, D., Duarte, M., Vaquero, C., and Gatignol, A. (2000). Analysis of a binding difference between the two dsRNA-binding domains in TRBP reveals the modular function of a KR-helix motif. Eur. J. Biochem. *267*, 2419–2431.

De Vito, C., Riggi, N., Cornaz, S., Suvà, M.L., Baumer, K., Provero, P., and Stamenkovic, I. (2012). A TARBP2-dependent miRNA expression profile underlies cancer stem cell properties and provides candidate therapeutic reagents in Ewing sarcoma. Cancer Cell *21*, 807–821.

Denli, A.M., Tops, B.B., Plasterk, R.H., Ketting, R.F., and Hannon, G.J. (2004). Processing of primary microRNAs by the Microprocessor complex. Nature *432*, 231–235.

Dorin, D., Bonnet, M.C., Bannwarth, S., Gatignol, A., Meurs, E.F., and Vaquero, C. (2003). The TAR RNA-binding protein, TRBP, stimulates the expression of TAR-containing RNAs in vitro and in vivo independently of its ability to inhibit the dsRNA-dependent kinase PKR. J. Biol. Chem. *278*, 4440–4448.

Fukunaga, R., Han, B.W., Hung, J.H., Xu, J., Weng, Z., and Zamore, P.D. (2012). Dicer partner proteins tune the length of mature miRNAs in flies and mammals. Cell *151*, 533–546.

Gatignol, A., Buckler-White, A., Berkhout, B., and Jeang, K.T. (1991). Characterization of a human TAR RNA-binding protein that activates the HIV-1 LTR. Science *251*, 1597–1600.

Gatignol, A., Duarte, M., Daviet, L., Chang, Y.N., and Jeang, K.T. (1996). Sequential steps in Tat trans-activation of HIV-1 mediated through cellular DNA, RNA, and protein binding factors. Gene Expr. *5*, 217–228.

Gatignol, A., Lainé, S., and Clerzius, G. (2005). Dual role of TRBP in HIV replication and RNA interference: viral diversion of a cellular pathway or evasion from antiviral immunity? Retrovirology *2*, 65.

Ghildiyal, M., Xu, J., Seitz, H., Weng, Z., and Zamore, P.D. (2010). Sorting of Drosophila small silencing RNAs partitions microRNA* strands into the RNA interference pathway. RNA *16*, 43–56.

Gregory, R.I., Yan, K.P., Amuthan, G., Chendrimada, T., Doratotaj, B., Cooch, N., and Shiekhattar, R. (2004). The Microprocessor complex mediates the genesis of microRNAs. Nature *432*, 235–240.

Grishok, A., Pasquinelli, A.E., Conte, D., Li, N., Parrish, S., Ha, I., Baillie, D.L., Fire, A., Ruvkun, G., and Mello, C.C. (2001). Genes and mechanisms related to RNA interference regulate expression of the small temporal RNAs that control C. elegans developmental timing. Cell *106*, 23–34.

Gupta, V., Huang, X., and Patel, R.C. (2003). The carboxy-terminal, M3 motifs of PACT and TRBP have opposite effects on PKR activity. Virology *315*, 283–291.

Ha, M., and Kim, V.N. (2014). Regulation of microRNA biogenesis. Nat. Rev. Mol. Cell Biol. *15*, 509–524.

Haase, A.D., Jaskiewicz, L., Zhang, H., Lainé, S., Sack, R., Gatignol, A., and Filipowicz, W. (2005). TRBP, a regulator of cellular PKR and HIV-1 virus expression, interacts with Dicer and functions in RNA silencing. EMBO Rep. *6*, 961–967.

Hammond, S.M., Boettcher, S., Caudy, A.A., Kobayashi, R., and Hannon, G.J. (2001). Argonaute2, a link between genetic and biochemical analyses of RNAi. Science *293*, 1146–1150.

Han, J., Lee, Y., Yeom, K.H., Kim, Y.K., Jin, H., and Kim, V.N. (2004). The Drosha-DGCR8 complex in primary microRNA processing. Genes Dev. *18*, 3016–3027.

Heo, I., Ha, M., Lim, J., Yoon, M.J., Park, J.E., Kwon, S.C., Chang, H., and Kim, V.N. (2012). Mono-uridylation of pre-microRNA as a key step in the biogenesis of group II let-7 microRNAs. Cell *151*, 521–532.

Hutvágner, G., McLachlan, J., Pasquinelli, A.E., Bálint, E., Tuschl, T., and Zamore, P.D. (2001). A cellular function for the RNA-interference enzyme Dicer in the maturation of the let-7 small temporal RNA. Science *293*, 834–838.

Ketting, R.F., Fischer, S.E., Bernstein, E., Sijen, T., Hannon, G.J., and Plasterk, R.H. (2001). Dicer functions in RNA interference and in synthesis of small RNA involved in developmental timing in C. elegans. Genes Dev. *15*, 2654–2659.

Khvorova, A., Reynolds, A., and Jayasena, S.D. (2003). Functional siRNAs and miRNAs exhibit strand bias. Cell *115*, 209–216.

Kim, Y., Kweon, J., Kim, A., Chon, J.K., Yoo, J.Y., Kim, H.J., Kim, S., Lee, C., Jeong, E., Chung, E., et al. (2013a). A library of TAL effector nucleases spanning the human genome. Nat. Biotechnol. *31*, 251–258.

Kim, Y.K., Wee, G., Park, J., Kim, J., Baek, D., Kim, J.S., and Kim, V.N. (2013b). TALEN-based knockout library for human microRNAs. Nat. Struct. Mol. Biol. *20*, 1458–1464.

Kim, H., Kim, M.S., Wee, G., Lee, C.I., Kim, H., and Kim, J.S. (2013c). Magnetic separation and antibiotics selection enable enrichment of cells with ZFN/TALEN-induced mutations. PLoS ONE *8*, e56476.

Kim, Y., Lee, J.H., Park, J.E., Cho, J., Yi, H., and Kim, V.N. (2014). PKR is activated by cellular dsRNAs during mitosis and acts as a mitotic regulator. Genes Dev. *28*, 1310–1322.

Knight, S.W., and Bass, B.L. (2001). A role for the RNase III enzyme DCR-1 in RNA interference and germ line development in Caenorhabditis elegans. Science *293*, 2269–2271.

Landthaler, M., Yalcin, A., and Tuschl, T. (2004). The human DiGeorge syndrome critical region gene 8 and Its D. melanogaster homolog are required for miRNA biogenesis. Curr. Biol. *14*, 2162–2167.

Laraki, G., Clerzius, G., Daher, A., Melendez-Peña, C., Daniels, S., and Gatignol, A. (2008). Interactions between the double-stranded RNA-binding

proteins TRBP and PACT define the Medipal domain that mediates protein-protein interactions. RNA Biol. *5*, 92–103.

Lee, H.Y., and Doudna, J.A. (2012). TRBP alters human precursor microRNA processing in vitro. RNA *18*, 2012–2019.

Lee, Y., Jeon, K., Lee, J.T., Kim, S., and Kim, V.N. (2002). MicroRNA maturation: stepwise processing and subcellular localization. EMBO J. *21*, 4663–4670.

Lee, Y., Ahn, C., Han, J., Choi, H., Kim, J., Yim, J., Lee, J., Provost, P., Rådmark, O., Kim, S., and Kim, V.N. (2003). The nuclear RNase III Drosha initiates microRNA processing. Nature *425*, 415–419.

Lee, J.Y., Kim, H., Ryu, C.H., Kim, J.Y., Choi, B.H., Lim, Y., Huh, P.W., Kim, Y.H., Lee, K.H., Jun, T.Y., et al. (2004). Merlin, a tumor suppressor, interacts with transactivation-responsive RNA-binding protein and inhibits its oncogenic activity. J. Biol. Chem. *279*, 30265–30273.

Lee, Y., Hur, I., Park, S.Y., Kim, Y.K., Suh, M.R., and Kim, V.N. (2006). The role of PACT in the RNA silencing pathway. EMBO J. *25*, 522–532.

Liu, Q., Rand, T.A., Kalidas, S., Du, F., Kim, H.E., Smith, D.P., and Wang, X. (2003). R2D2, a bridge between the initiation and effector steps of the Drosophila RNAi pathway. Science *301*, 1921–1925.

Liu, X., Jiang, F., Kalidas, S., Smith, D., and Liu, Q. (2006). Dicer-2 and R2D2 coordinately bind siRNA to promote assembly of the siRISC complexes. RNA *12*, 1514–1520.

MacRae, I.J., Ma, E., Zhou, M., Robinson, C.V., and Doudna, J.A. (2008). In vitro reconstitution of the human RISC-loading complex. Proc. Natl. Acad. Sci. USA *105*, 512–517.

Melo, S.A., Ropero, S., Moutinho, C., Aaltonen, L.A., Yamamoto, H., Calin, G.A., Rossi, S., Fernandez, A.F., Carneiro, F., Oliveira, C., et al. (2009). A TARBP2 mutation in human cancer impairs microRNA processing and DICER1 function. Nat. Genet. *41*, 365–370.

Meurs, E.F., Watanabe, Y., Kadereit, S., Barber, G.N., Katze, M.G., Chong, K., Williams, B.R., and Hovanessian, A.G. (1992). Constitutive expression of human double-stranded RNA-activated p68 kinase in murine cells mediates phosphorylation of eukaryotic initiation factor 2 and partial resistance to encephalomyocarditis virus growth. J. Virol. *66*, 5805–5814.

Mourelatos, Z., Dostie, J., Paushkin, S., Sharma, A., Charroux, B., Abel, L., Rappsilber, J., Mann, M., and Dreyfuss, G. (2002). miRNPs: a novel class of ribonucleoproteins containing numerous microRNAs. Genes Dev. *16*, 720–728.

Noland, C.L., and Doudna, J.A. (2013). Multiple sensors ensure guide strand selection in human RNAi pathways. RNA *19*, 639–648.

Noland, C.L., Ma, E., and Doudna, J.A. (2011). siRNA repositioning for guide strand selection by human Dicer complexes. Mol. Cell *43*, 110–121.

Offermann, M.K., Zimring, J., Mellits, K.H., Hagan, M.K., Shaw, R., Medford, R.M., Mathews, M.B., Goodbourn, S., and Jagus, R. (1995). Activation of the double-stranded-RNA-activated protein kinase and induction of vascular cell adhesion molecule-1 by poly (I).poly (C) in endothelial cells. Eur. J. Biochem. *232*, 28–36.

Olsen, J.V., Vermeulen, M., Santamaria, A., Kumar, C., Miller, M.L., Jensen, L.J., Gnad, F., Cox, J., Jensen, T.S., Nigg, E.A., et al. (2010). Quantitative phosphoproteomics reveals widespread full phosphorylation site occupancy during mitosis. Sci. Signal. *3*, ra3.

Park, H., Davies, M.V., Langland, J.O., Chang, H.W., Nam, Y.S., Tartaglia, J., Paoletti, E., Jacobs, B.L., Kaufman, R.J., and Venkatesan, S. (1994). TAR RNA-binding protein is an inhibitor of the interferon-induced protein kinase PKR. Proc. Natl. Acad. Sci. USA *91*, 4713–4717.

Park, J.E., Heo, I., Tian, Y., Simanshu, D.K., Chang, H., Jee, D., Patel, D.J., and Kim, V.N. (2011). Dicer recognizes the 5′ end of RNA for efficient and accurate processing. Nature *475*, 201–205.

Paroo, Z., Ye, X., Chen, S., and Liu, Q. (2009). Phosphorylation of the human microRNA-generating complex mediates MAPK/Erk signaling. Cell *139*, 112–122.

Patel, R.C., and Sen, G.C. (1998). PACT, a protein activator of the interferon-induced protein kinase, PKR. EMBO J. *17*, 4379–4390.

Patel, R.C., Stanton, P., McMillan, N.M., Williams, B.R., and Sen, G.C. (1995). The interferon-inducible double-stranded RNA-activated protein kinase self-associates in vitro and in vivo. Proc. Natl. Acad. Sci. USA *92*, 8283–8287.

Ribas, V.T., Gonçalves, B.S., Linden, R., and Chiarini, L.B. (2012). Activation of c-Jun N-terminal kinase (JNK) during mitosis in retinal progenitor cells. PLoS ONE *7*, e34483.

Sanghvi, V.R., and Steel, L.F. (2011). The cellular TAR RNA binding protein, TRBP, promotes HIV-1 replication primarily by inhibiting the activation of double-stranded RNA-dependent kinase PKR. J. Virol. *85*, 12614–12621.

Schwarz, D.S., Hutvágner, G., Du, T., Xu, Z., Aronin, N., and Zamore, P.D. (2003). Asymmetry in the assembly of the RNAi enzyme complex. Cell *115*, 199–208.

Singh, M., Castillo, D., Patel, C.V., and Patel, R.C. (2011). Stress-induced phosphorylation of PACT reduces its interaction with TRBP and leads to PKR activation. Biochemistry *50*, 4550–4560.

Tabara, H., Sarkissian, M., Kelly, W.G., Fleenor, J., Grishok, A., Timmons, L., Fire, A., and Mello, C.C. (1999). The rde-1 gene, RNA interference, and transposon silencing in C. elegans. Cell *99*, 123–132.

Takada, Y., Ichikawa, H., Pataer, A., Swisher, S., and Aggarwal, B.B. (2007). Genetic deletion of PKR abrogates TNF-induced activation of IkappaBalpha kinase, JNK, Akt and cell proliferation but potentiates p44/p42 MAPK and p38 MAPK activation. Oncogene *26*, 1201–1212.

Tomari, Y., Matranga, C., Haley, B., Martinez, N., and Zamore, P.D. (2004). A protein sensor for siRNA asymmetry. Science *306*, 1377–1380.

Tomari, Y., Du, T., and Zamore, P.D. (2007). Sorting of Drosophila small silencing RNAs. Cell *130*, 299–308.

Topham, C.H., and Taylor, S.S. (2013). Mitosis and apoptosis: how is the balance set? Curr. Opin. Cell Biol. *25*, 780–785.

Yang, X., Nath, A., Opperman, M.J., and Chan, C. (2010). The double-stranded RNA-dependent protein kinase differentially regulates insulin receptor substrates 1 and 2 in HepG2 cells. Mol. Biol. Cell *21*, 3449–3458.

Zamanian-Daryoush, M., Der, S.D., and Williams, B.R. (1999). Cell cycle regulation of the double stranded RNA activated protein kinase, PKR. Oncogene *18*, 315–326.

Zhang, H., Kolb, F.A., Jaskiewicz, L., Westhof, E., and Filipowicz, W. (2004). Single processing center models for human Dicer and bacterial RNase III. Cell *118*, 57–68.

Zhong, J., Peters, A.H., Lee, K., and Braun, R.E. (1999). A double-stranded RNA binding protein required for activation of repressed messages in mammalian germ cells. Nat. Genet. *22*, 171–174.